Int. J. Heat Mass Transfer. Vol. 16, pp. 611–627. Pergamon Press 1973. Printed in Great Britain

A THEORETICAL STUDY OF NATURAL CONVECTION HEAT TRANSFER FROM DOWNWARD-FACING HORIZONTAL SURFACES WITH UNIFORM HEAT FLUX

TETSU FUJII, HIROSHI HONDA and ITSUKI MORIOKA

Research Institute of Industrial Science, Kyushu University, Fukuoka, Japan

(*Received* 6 *November* 1971)

Abstract—The paper treats of a theoretical study on steady laminar natural convection along a horizontal plate, which is heated with uniform heat flux and facing downwards. The boundary layer equations are solved by an approximate integral treatment, based on a concept of minimum boundary layer thickness which is derived from the consideration on the time evolution of unsteady flow field.

While the solutions for an infinite strip and a circular plate are obtained analytically for any Prandtl numbers, the solution for a rectangular plate is obtained for the case of $Pr \to \infty$ only. Approximate solutions by Galerkin's method are also obtained for these three plates. The agreement found between the analytical and approximate solutions is fairly good, especially in the case of $Pr \to \infty$.

Local Nusselt number Nu_x is proportional to one-sixth power of modified Grashof number, whereas average Nusselt number Nu is proportional to one-fifth power of Grashof number. The value of $Nu/Ra^{\frac{1}{5}}$ increases with the increase of Prandtl number up to $Pr = 100$, becoming almost constant in the range of $Pr > 100$. Besides, it is the smallest for an infinite strip, and becomes larger toward a rectangular plate and a circular plate.

NOMENCLATURE

a, one-half of the width of an infinite strip, or one-half of one side of a rectangular plate, or the radius of a circular plate;

b, one-half of the other side of a rectangular plate;

c, one side of the rectangular domain shown in Fig. 1;

A, B, D, constants defined by (19);

C, coefficient $= Nu/Ra^{\frac{1}{5}}$ or $Nu/Ra^{\frac{1}{4}}$;

c_v, specific heat at constant volume;

g, gravitational acceleration;

Gr, Grashof number defined by (32);

Gr^*, modified Grashof number defined by (16);

L, aspect ratio of a rectangular plate $= b/a$;

m, n, constants defined by (24);

Nu_x, Nu_{xz}, local Nusselt number defined by (29);

Nu, average Nusselt number defined by (31), (48) and (66);

p, static pressure;

p^*, difference between local pressure and gravitational potential, defined by (5);

Pr, Prandtl number;

q, heat flux at the plate surface;

Q, heat flux defined by (14);

Ra, Rayleigh number $= GrPr$;

Ra^*, modified Rayleigh number $= Gr^*Pr$;

t, time;

T, temperature;

ΔT, temperature difference $= T - T_\infty$;

ΔT_{av}, average temperature difference defined by (33), (49) and (67);

u, v, w, velocity components in x-, y- and z-direction respectively;

u_x, u_{xz}, v_{xz}, velocity component defined in (12), (55) and (56) respectively;

V, rectangular domain shown in Fig. 1;

x, y, z, coordinates defined in Fig. 1.

Greek symbols

α_x, α, local and average heat-transfer coefficients defined in (29) and (31) respectively;
β, average volumetric thermal expansion coefficient;
γ, γ', constants defined by (23) and (47) respectively;
δ, boundary layer thickness;
Δ, normalized boundary-layer thickness defined by (22);
η, independent variable defined by (13);
$\theta(\eta)$, temperature profile defined in (11);
$\varkappa$, thermal diffusivity;
λ, thermal conductivity;
ν, kinematic viscosity;
ρ, density;
$\varphi(\eta)$, velocity profile defined in (12);
Φ, local potential defined in (37);
Ψ, function defined by (35).

Subscripts

a, conditions at $x = a$;
c, conditions at $y = c$;
m, minimum value;
w, conditions at the plate surface;
0, conditions at the plate center or conditions at $y = 0$;
1, conditions at $\bar{x} = 1$;
∞, conditions in the ambient fluid.

Superscripts

$\bar{}$, dimensionless variable;
$'$, unsteady state.

1. INTRODUCTION

THERE are a good many experimental and theoretical studies made on the natural convection about a horizontal surface of finite size. When the heated surface is facing downwards, the flow of fluid within the boundary layer is directed toward the edges of the surface, whereas the flow is reversed when the surface is facing upwards. The characteristics of natural convection in these two cases are quite different from each other. The subject considered in this paper is confined to the problem of laminar boundary layer flow along a heated horizontal plate facing downwards or that along a cooled plate facing upwards.

Weise [1] experimented on heat transfer from heated square plates to air, and recommended the relation $Nu = 0{\cdot}47\ Ra^{\frac{1}{4}}$ at $Ra \doteqdot 10^7$ for the heat transfer coefficient, which was averaged over the whole surface. The measured temperature distribution and Schlieren photograph showed that the thermal boundary layer along the lower surface took maximum thickness at the center and that its thickness decreased toward the plate edges. Saunders *et al.* [2] estimated the heat transfer coefficient for a heated rectangular plate in air, by measuring the refraction of parallel light beam passing close to the surface. Kraus [3] measured distributions of temperature and velocity of air about heated square plates, and found that Nusselt number, which was averaged over the whole surface, was proportioned to one-third power of Rayleigh number.

Fishenden–Saunders [4] recommended an experimental curve for the heat transfer from a horizontal square plate facing downwards to air, and proposed the relation $Nu = 0{\cdot}21\ Ra^{\frac{1}{4}}$ in the range of $1{\cdot}3 \times 10^4 < Ra < 4 \times 10^9$. Stewartson [11] reexamined the data of Fishenden–Saunders and proposed the relation $Nu = 0{\cdot}614\ Ra^{\frac{1}{4}}$. Birkebak–Abdulkadir [5] measured distributions of temperature and velocity of water about a square plate with uniform surface heat flux. The temperature distribution was shown to take a similar profile. The velocity distribution was caught by photographing the movement of plastic particles of neutral density which were dispersed in the ambient fluid. Outside the boundary layer, the particles moved inward towards the direction of centerline, turned upward, entered the boundary layer from below and finally moved sideways toward the plate edges following the boundary layer flow. A velocity

profile obtained by the electrolysis of tellurium in water was in good agreement with that assumed by Singh *et al.* [15]. The heat transfer coefficient was correlated as $Nu = 0{\cdot}681\ Ra^{\frac{1}{4}}$ in the range of $3 \times 10^8 < Ra < 10^9$, where the area averaged wall temperature was used as the representative one.

Fujii–Imura [6] experimented on heat transfer from inclined plates to water and obtained data on the horizontal surface facing downwards as a particular case. The boundary layers along the test surfaces were restricted two-dimensionally. The heat transfer coefficient was correlated as $Nu = 0{\cdot}44\ Ra^{\frac{1}{4}}$ in the range of $3 \times 10^5 < Ra < 1{\cdot}5 \times 10^{10}$. When the plates were made to incline a few degrees from the horizontal, the relation changed to $Nu = C\,Ra^{\frac{1}{4}}$. The change of heat transfer characteristics mentioned above was ascribed to the change of flow pattern; that is, the photographs of flow field, which was visualized by the use of floated aluminium particles, disclosed the fact that the same flow pattern as described by Birkebak–Abdulkadir [5] changed to the flow pattern, which originated at the lower edge and moved upwards, in consequence of the slight surface inclination. Aihara *et al.* [7] measured the temperature and velocity distribution in the two-dimensional boundary layer of air about a rectangular plate. The results are referred later in section 5.

Most of the theoretical works concerning horizontal plates were based on the boundary layer theory approximation. Sugawara–Michiyoshi [8] presented the analysis for an infinite strip of finite thickness, replacing its cross section for a very thin ellipse and taking the component of buoyancy parallel to the heated surface as the driving force of convection. The heat transfer coefficient was expressed as $Nu = C\,Ra^{\frac{1}{4}}$, where C depended on the ratio of major to minor radius of the ellipse. The distribution of local heat-transfer coefficient was in good agreement with Weise's [1] experimental results, provided that the ratio was assumed as equal to ten.

Levy [9] proposed a solution for a heated infinite strip facing upwards by the approximate integral treatment. The pressure gradient along the plate was retained in the equations of motion, and the boundary layer was assumed to originate at the plate edges and grow inward. Wagner [10] solved Levy's integral equations for the case of an infinite strip facing downwards, by assuming that the boundary layer thickness is equal to zero at the plate edges. Since the pressure terms were eliminated from the equations of motion by differentiating them, the inertia terms did not contribute to the solution of Wagner. The heat transfer coefficient was expressed as $Nu = 0{\cdot}5\,Ra^{\frac{1}{4}}$.

Stewartson [11] sought similarity transformation of the basic equations and obtained a numerical solution for an infinite strip for $Pr = 0{\cdot}72$, which was expressed as $Nu = 0{\cdot}603\ Ra^{\frac{1}{4}}$. As pointed by Gill *et al.* [12], Yamagata [13] and Rotem [14], however, Stewartson committed sign errors in his calculation and his results actually correspond to the case of a heated plate facing upward. Yamagata [13] derived a solution by the approximate integral treatment for an infinite strip. The boundary-layer thickness was put equal to zero at the point $x/a = 1{\cdot}1$, so that its distribution along the width might agree with Weise's [1] experimental result. The heat transfer coefficient was expressed as $Nu = 0{\cdot}62\ Ra^{\frac{1}{4}}$. Singh *et al.* [15] solved Wagner's integral equations by Ritz's and/or Galerkin's approximate methods for the cases of an infinite strip, a circular and a rectangular plate. Nusselt number was proved to be proportional to one-fifth power of Rayleigh number in each case.

Clifton–Chapman [16] introduced the minimum mechanical energy principle, which was established in the open channel hydraulics, in order to determine the boundary layer thickness at the plate edge. The pressure terms were eliminated from the momentum equations by integrating them across the boundary layer, and, therefore, the contribution of inertia terms were retained in the resulting equation. The heat-transfer coefficient for an infinite strip was expressed as $Nu = C\,Ra^{\frac{1}{4}}$. The thickness of the

boundary layer and the coefficient C were represented graphically as a function of Prandtl number. Singh–Birkebak [17] proposed a solution of an infinite strip, introducing a new concept that the boundary layer thickness has singular points at the plate edges. This solution suggests that the boundary layer thickness takes the minimum value. The boundary-layer thickness and the heat-transfer coefficient have the dependency upon Rayleigh number and Prandtl number similar to those of Clifton–Chapman.

Chen [18] treated the problem for an infinite strip as a stagnation-point flow. The similarity transformation was sought and the resulting set of ordinary differential equations were solved numerically. The momentum equation retained the buoyancy term along the strip and the heat transfer coefficient was expressed as $Nu = C\,Ra^{\frac{1}{4}}$. Suriano–Yang [19] solved the same problem by a numerical finite-difference scheme in the Rayleigh number range up to 37·5 for two Prandtl number of 0·72 and 10. From Table 1 of [19], the heat transfer coefficient can be expressed as $Nu = C(Pr)\,Ra^n$ in the range of $5 < Ra < 37{\cdot}5$, where the index n is larger than $\frac{1}{3}$ and takes different value for two Prandtl numbers. The figure of n seems to be too large, because it is considered in reference to the experimental results on natural convection for the other geometrical configuration that the figure decreases with decrease of Rayleigh number.

The literature survey mentioned above reveals the following facts. Firstly, experimental observations disclose that a laminar boundary layer is formed along a heated horizontal plate facing downwards and that the thickness of the boundary layer is maximum at the plate center and decreases with flowing toward downstream, i.e. the plate edges. The temperature distribution in the boundary layer is considered to be similar except the immediate neighbourhood of the plate edge. Secondly, the indication of theoretical studies are that similarity solution technique is not applicable to the present problem. This is because the present boundary layer does not satisfy the fundamental requirement of similarity that the boundary layer should grow towards the downstream. Thus, the method of theoretical analysis may be confined to the numerical finite difference scheme or the approximate integral treatment. Thirdly, when the approximate integral treatment is applied to the present problem, there arises an important question how to put the boundary conditions at the plate edge. Though Yamagata [13], Clifton–Chapman [16] and Singh–Birkebak [17] proposed new concepts to determine the boundary layer thickness, they did not present any sufficient consideration upon the adequacy. The accuracy of the approximate solution by Galerkin's method is not yet estimated. Finally, it may be pointed out that the theoretical study in which the component of buoyancy along the plate is introduced into momentum equation as the driving force of convection gives the expression for average heat transfer coefficient as $Nu = C\,Ra^{\frac{1}{4}}$, whereas the study in which the pressure gradient along the plate is taken into account gives the expression as $Nu = C\,Ra^{\frac{1}{4}}$.

The aim of the present paper is to solve these questions analytically. Here only the case of uniform surface heat flux has been treated, because the case has been hitherto overlooked by most authors and because the analytical treatment is rather manageable. The numerical evaluations are made for an infinite strip, a circular plate and a square plate.

2. THE SOLUTION FOR AN INFINITE STRIP

The coordinate system is shown in Fig. 1, where a, T_w, T_∞, and q represent half width of the strip, surface temperature, ambient fluid temperature and surface heat flux respectively. When the laminar boundary layer approximation is assumed to be possible, the equations of the steady state conservation of mass, momentum and energy can be described as follows;

$$\frac{\partial u}{\partial x} + \frac{\partial v}{\partial y} = 0, \tag{1}$$

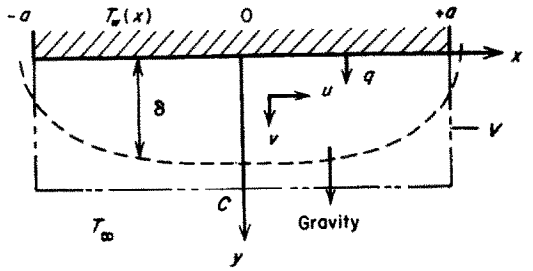

FIG. 1. Coordinate system: in the case of circular plate, x-coordinate denotes radial one; in the case of rectangular plate, z-coordinate is taken perpendicularly to the x–y plane.

$$u\frac{\partial u}{\partial x}+v\frac{\partial u}{\partial y}=-\frac{1}{\rho}\frac{\partial p^*}{\partial x}+\nu\frac{\partial^2 u}{\partial y^2}, \tag{2}$$

$$0=-\frac{1}{\rho}\frac{\partial p^*}{\partial y}-g\beta(T-T_\infty), \tag{3}$$

$$u\frac{\partial T}{\partial x}+v\frac{\partial T}{\partial y}=\varkappa\frac{\partial^2 T}{\partial y^2}, \tag{4}$$

where

$$p^*=p-\rho_\infty gy. \tag{5}$$

The boundary conditions are

$$y=0; \qquad u=v=0, \quad -\lambda(\partial T/\partial y)_0=q, \tag{6}$$

$$y\to\infty; \qquad u\to 0, \quad T\to T_\infty, \quad p^*\to 0. \tag{7}$$

Substituting p^*, which is obtained by integrating (3) from y to ∞ with respect to y, into (2), we obtain

$$u\frac{\partial u}{\partial x}+v\frac{\partial u}{\partial y}=g\beta\frac{\partial}{\partial x}\int_y^\infty (T-T_\infty)\,dy+\nu\frac{\partial^2 u}{\partial y^2}, \tag{8}$$

where both boundary layers of temperature and velocity are assumed to be of the same thickness δ. Integrating (4) and (8) from 0 to δ with respect to y under new assumptions $\partial u/\partial y=0$ and $\partial T/\partial y=0$ at $y=\delta$, and eliminating v by using (1), we obtain

$$\frac{d}{dx}\int_0^\delta u^2\,dy=-g\beta\frac{d}{dx}\int_0^\delta dy\int_y^\delta (T-T_\infty)\,dy-\nu\left(\frac{\partial u}{\partial y}\right)_0, \tag{9}$$

$$\frac{d}{dx}\int_0^\delta u(T-T_\infty)\,dy=\frac{\varkappa g}{\lambda}. \tag{10}$$

By assuming similar profiles of temperature and velocity such as

$$T-T_\infty=Q\theta(\eta)\,\delta, \tag{11}$$

$$u=u_x\varphi(\eta), \tag{12}$$

where

$$\eta=y/\delta, \tag{13}$$

$$Q=-q(d\theta/d\eta)_0/\lambda, \tag{14}$$

and by introducing dimensionless variables such as

$$\bar{x}=x/a, \qquad \bar{\delta}=\delta(Gr^*Pr)^{\frac{1}{4}}/a,$$

$$\bar{u}_{\bar{x}}=u_x a(Gr^*Pr)^{-\frac{1}{2}}/\varkappa, \tag{15}$$

where

$$Gr^*=a^4g\beta q/\nu^2\lambda=-(d\theta/d\eta)_0 a^4g\beta Q/\nu^2, \tag{16}$$

(9) and (10) are reduced to

$$\frac{1}{Pr}\frac{d}{d\bar{x}}(\bar{\delta}\bar{u}_x^2)=-A\frac{d\bar{\delta}^3}{d\bar{x}}-B\frac{\bar{u}_{\bar{x}}}{\bar{\delta}}, \tag{17}$$

$$\frac{d}{d\bar{x}}(\bar{\delta}^2\bar{u}_{\bar{x}})=D, \tag{18}$$

where

$$A=\frac{\int_0^1 d\eta\int_\eta^1\theta\,d\eta}{-(d\theta/d\eta)_0\int_0^1\varphi^2\,d\eta}, \qquad B=\frac{(d\varphi/d\eta)_0}{\int_0^1\varphi^2\,d\eta},$$

$$D=\frac{-(d\theta/d\eta)_0}{\int_0^1\theta\varphi\,d\eta}. \tag{19}$$

Since dimensionless boundary layer thickness $\bar{\delta}$ is considered to be symmetric with respect to the axis $\bar{x}=0$, and since we cannot suppose any reason why $\bar{\delta}$ changes abruptly, it is reasonable to assume

$$\bar{x} = 0;\ \mathrm{d}\bar{\delta}/\mathrm{d}\bar{x} = 0. \tag{20}$$

The solution of (17) and (18) subject to condition (20) is obtained analytically as

$$\Delta^{\gamma} - \Delta^{6} = n\left(1 + \frac{1}{mPr}\right)\frac{\bar{x}^2}{\bar{\delta}_0^6}, \tag{21}$$

where

$$\Delta = \bar{\delta}/\bar{\delta}_0, \quad \gamma = 6/(2 + mPr), \tag{22),(23}$$

$$m = \frac{(\mathrm{d}\varphi/\mathrm{d}\eta)_0 \int_0^1 \theta\varphi\,\mathrm{d}\eta}{-(\mathrm{d}\theta/\mathrm{d}\eta)_0 \int_0^1 \varphi^2\,\mathrm{d}\eta},$$

$$n = \frac{(\mathrm{d}\theta/\mathrm{d}\eta)_0^2\,(\mathrm{d}\varphi/\mathrm{d}\eta)_0}{\int_0^1 \mathrm{d}\eta \int_\eta^1 \theta\,\mathrm{d}\eta \cdot \int_0^1 \theta\varphi\,\mathrm{d}\eta}. \tag{24}$$

Since the boundary-layer thickness at the plate center $\bar{\delta}_0$ in (21) still remains undetermined, one more condition is required.

2.1 *The solution subject to the assumption of minimum boundary layer thickness*

An assumption of minimum boundary layer thickness is introduced in order to determine the boundary layer profile. Substituting $\bar{\delta} = \bar{\delta}_1$ and $\Delta = \Delta_1$ at $\bar{x} = 1$ into (21), we obtain

$$\bar{\delta}_0^6 = n\left(1 + \frac{1}{mPr}\right)\frac{1}{(\Delta_1^{\gamma} - \Delta_1^6)}. \tag{25}$$

$\bar{\delta}_0$ takes the minimum value $\bar{\delta}_{0m}$ at $\Delta_1 = \Delta_{1m}$, where

$$\bar{\delta}_{0m} = \left[\frac{n(1 + 1/mPr)}{\Delta_{1m}^{\gamma} - \Delta_{1m}^6}\right]^{\frac{1}{6}},$$

$$\Delta_{1m} = (2 + mPr)^{-1/(6-\gamma)}. \tag{26}$$

Substitution of $\bar{\delta}_0 = \bar{\delta}_{0m}$ into (21) yields the relation between the local boundary-layer thickness $\Delta = \Delta_m$ and $\bar{x}$.

Differentiation of (21) with respect to $\bar{x}$ leads to

$$\frac{\mathrm{d}\Delta_m}{\mathrm{d}\bar{x}} = \frac{2n}{\bar{\delta}_{0m}^6}\left(1 + \frac{1}{mPr}\right)\frac{\bar{x}\Delta_m}{\gamma\Delta_m^{\gamma} - 6\Delta_m^6}. \tag{27}$$

Then it follows

$$(\mathrm{d}\Delta_m/\mathrm{d}\bar{x})_{x=\pm 1} = \mp\infty. \tag{28}$$

Thus, the assumption of minimum boundary layer thickness seems to be equivalent in effect to the assumption expressed by (28), as proposed by Singh–Birkebak [17] in their determination of the boundary-layer thickness for the infinite strip with uniform surface temperature.

Local Nusselt number Nu_x is expressed as

$$Nu_x = \frac{\alpha_x a}{\lambda} = \frac{qa}{\Delta T_w \lambda} = \frac{-(\mathrm{d}\theta/\mathrm{d}\eta)_0}{\bar{\delta}_{0m}}(Gr^*Pr)^{\frac{1}{4}}\frac{1}{\Delta_m}, \tag{29}$$

where

$$\Delta T_w = T_w(x) - T_\infty. \tag{30}$$

For the convenience of comparing the present result with that for uniform surface temperature, average Nusselt number Nu is defined as follows:

$$Nu = \frac{\alpha a}{\lambda} = \frac{qa}{\Delta T_{av}\lambda} = \left[\frac{-(\mathrm{d}\theta/\mathrm{d}\eta)_0}{\bar{\delta}_{0m}\int_0^1 \Delta_m\,\mathrm{d}\bar{x}}\right]^{\frac{1}{4}}(GrPr)^{\frac{1}{4}}, \tag{31}$$

where

$$Gr = a^3 g\beta\Delta T_{av}/\nu^2, \quad \Delta T_{av} = \int_0^a \Delta T_w\,\mathrm{d}x/a. \tag{32),(33}$$

2.2 *Physical interpretation of the assumption of minimum boundary layer thickness*

Glansdorff–Prigogine [20] have established a general evolution criterion valid for the whole class of macroscopic systems and derived a variational principle, in which the steady state of the system is represented in the light of local potential. For the present problem, the local potential is derived by following the technique presented by Schechter–Himmelblau [21].

A rectangular domain V, where the boundary layer along the heated plate is included as shown in Fig. 1, is introduced here. The pertinent equations are

$$\frac{\partial u'}{\partial x} + \frac{\partial v'}{\partial y} = 0, \tag{1)'}$$

$$\frac{\partial u'}{\partial t} + u'\frac{\partial u'}{\partial x} + v'\frac{\partial u'}{\partial y} = -\frac{1}{\rho}\frac{\partial p^{*\prime}}{\partial x} + \nu\frac{\partial^2 u'}{\partial y^2}, \quad (2)'$$

$$\frac{\partial v'}{\partial t} = -\frac{1}{\rho}\frac{\partial p^{*\prime}}{\partial y} - g\beta(T' - T_\infty), \quad (3)'$$

$$\frac{\partial T'}{\partial x} + u'\frac{\partial T'}{\partial x} + v'\frac{\partial T'}{\partial y} = \varkappa\frac{\partial^2 T'}{\partial y^2}, \quad (4)'$$

where

$$p^{*\prime} = p' - \rho_\infty g y, \quad (5)$$

and the prime denotes unsteady state. Multiplying (1)′–(4)′ by $\partial p'/\partial t$, $\rho\partial u'/\partial t$, $\rho\partial v'/\partial t$ and $(\rho c_v/T_\infty)\partial T'/\partial t$ respectively and then summing up the resultant equations, we obtain

$$\Psi = \left(\frac{\partial u'}{\partial x} + \frac{\partial v'}{\partial y}\right)\frac{\partial P^{*\prime}}{\partial t} + \rho\left(u'\frac{\partial u'}{\partial x} + v'\frac{\partial u'}{\partial y}\right) \times \frac{\partial u'}{\partial t} + \left(\frac{\partial p^{*\prime}}{\partial x}\frac{\partial u'}{\partial t} + \frac{\partial p^{*\prime}}{\partial y}\frac{\partial v'}{\partial t}\right) - \rho\nu\frac{\partial^2 u'}{\partial y^2}\frac{\partial u'}{\partial t} + \rho g\beta(T' - T_\infty)\frac{\partial v'}{\partial t} + \frac{\rho c_v}{T_\infty}\left(u'\frac{\partial T'}{\partial x} + v'\frac{\partial T'}{\partial y}\right) \times \frac{\partial T'}{\partial t} - \frac{\rho c_v \varkappa}{T_\infty}\frac{\partial^2 T'}{\partial y^2}\frac{\partial T'}{\partial t} \quad (34)$$

where Ψ is defined by

$$\Psi = -\left[\rho\left(\frac{\partial u'}{\partial t}\right)^2 + \rho\left(\frac{\partial v'}{\partial t}\right)^2 + \frac{\rho c_v}{T_\infty}\left(\frac{\partial T'}{\partial t}\right)^2\right]. \quad (35)$$

The function Ψ is of negative quadratic form and, therefore always nonpositive. By integrating the function Ψ over the volume V after partial integration,

$$\int_V \Psi\,dV = \int_V \left\{\left(\frac{\partial u'}{\partial x} + \frac{\partial v'}{\partial y}\right)\frac{\partial p^{*\prime}}{\partial t} + \frac{\rho}{2}\left(u'\frac{\partial^2 u'^2}{\partial t\partial x} + v'\frac{\partial^2 u'^2}{\partial t\partial y}\right) - \rho\left(u'^2\frac{\partial^2 u'}{\partial t\partial x} + u'v'\frac{\partial^2 u'}{\partial t\partial y}\right) + \left(\frac{\partial p^{*\prime}}{\partial x}\frac{\partial u'}{\partial t} + \frac{\partial p^{*\prime}}{\partial y}\frac{\partial v'}{\partial t}\right) + \frac{\rho\nu}{2}\frac{\partial}{\partial t}\left(\frac{\partial u'}{\partial y}\right)^2 + \rho g\beta(T' - T_\infty)\frac{\partial v'}{\partial t} + \frac{\rho c_v}{T_\infty}\left(u'\frac{\partial T'}{\partial x} + v'\frac{\partial T'}{\partial y}\right) \times \frac{\partial T'}{\partial t} + \frac{\rho c_v \varkappa}{2T_\infty}\frac{\partial}{\partial t}\left(\frac{\partial T'}{\partial y}\right)^2\right\} dV + \int_{-a}^{a}\left\{-\left(\rho\nu\frac{\partial u'}{\partial y}\frac{\partial u'}{\partial t} + \frac{\rho c_v \varkappa}{T_\infty}\frac{\partial T'}{\partial y}\frac{\partial T'}{\partial t}\right)_{y=0}^{y=c}\right\} \times dx \leqslant 0. \quad (36)$$

When the above integral is calculated in the neighbourhood of the steady state (u, v, p^*, T), functional coefficients of time derivatives in the integrand of (36) may be replaced by those values at the steady state as a first approximation. Thus

$$\int_V \Psi\,dV = \frac{\partial}{\partial t}\left[\int_V \left\{\left(\frac{\partial u}{\partial x} + \frac{\partial v}{\partial y}\right)p^{*\prime} + \frac{\rho}{2}\left(u\frac{\partial u'^2}{\partial x} + v\frac{\partial u'^2}{\partial y}\right) - \rho\left(u^2\frac{\partial u'}{\partial x} + uv\frac{\partial u'}{\partial y}\right) + \left(\frac{\partial p^*}{\partial x}u' + \frac{\partial p^*}{\partial y}v'\right) + \frac{\rho\nu}{2}\left(\frac{\partial u'}{\partial y}\right)^2 + \rho g\beta \times (T - T_\infty)v'\frac{\rho c_v}{T_\infty}\left(u\frac{\partial T}{\partial x} + v\frac{\partial T}{\partial y}\right)T' + \frac{\rho c_v \varkappa}{2T_\infty} \times \left(\frac{\partial T'}{\partial y}\right)^2\right\} dV + \int_{-a}^{a}\left\{-\left(\rho\nu\frac{\partial u}{\partial y}u' + \frac{\rho c_v \varkappa}{T_\infty} \times \frac{\partial T}{\partial y}T'\right)_{y=0}^{y=c}\right\} dx\right] \leqslant 0. \quad (36)'$$

When the quantity Φ is defined by

$$\int_V \Psi\,dV = \partial\Phi/\partial t, \quad (37)$$

Φ corresponds to the local potential introduced by Glansdorff–Prigogine. Since Φ can be decreased in time only, the local potential takes on a minimum value under a steady state.

The variation $\delta\Phi$ of local potential Φ, which is subject to the solution calculated from (21), becomes

$$\delta\Phi = \int_V \left[\left\{\rho\left(u\frac{\partial u'}{\partial x} + \frac{\partial u'}{\partial y}\right) + \frac{\partial p^*}{\partial x} - \rho\nu\frac{\partial^2 u'}{\partial y^2}\right\} \times \delta u' + \frac{\rho c_v}{T_\infty}\left(u\frac{\partial T}{\partial x} + v\frac{\partial T}{\partial y} - \varkappa\frac{\partial^2 T'}{\partial y^2}\right)\delta T'\right] dV$$

$$- \int_a^a \left[\left\{ \rho\nu \left(\frac{\partial u}{\partial y} - \frac{\partial u'}{\partial y} \right) \delta u' + \frac{pc_v\varkappa}{T_\infty} \times \left(\frac{\partial T}{\partial y} - \frac{\partial T'}{\partial y} \right) \delta T' \right\}_{y=0}^{y=c} \right] \mathrm{d}x. \quad (38)$$

Thus

$$\left(\frac{\delta \Phi}{\delta \delta} \right)_{\delta'=\delta} = \rho\varkappa^3 D^3 \int_0^1 \left(\varphi^2 - \frac{\mathrm{d}\varphi}{\mathrm{d}\eta} \int_0^\eta \varphi \, \mathrm{d}\eta \right) \times (\bar{\varphi} - 2\varphi) \, \mathrm{d}\eta \int_0^a \frac{x^2}{\delta^6} \left(1 - \frac{2x}{\delta} \frac{\mathrm{d}\delta}{\mathrm{d}x} \right) \mathrm{d}x$$

$$- 2\rho g \beta Q \varkappa D \int_0^1 (\bar{\varphi} - 2\bar{\varphi}) \int_\eta^1 \theta \, \mathrm{d}\eta \, \mathrm{d}\eta \int_0^a \times \frac{x}{\delta} \frac{\mathrm{d}\delta}{\mathrm{d}x} \mathrm{d}x - \rho\nu\varkappa^2 D^2 \int_0^1 \frac{\mathrm{d}^2\varphi}{\mathrm{d}\eta^2} (\bar{\varphi} - 2\varphi) \, \mathrm{d}\eta$$

$$\times \int_0^a \frac{x^2}{\delta^6} \mathrm{d}x + \frac{\rho c_v Q^2 \varkappa}{T_\infty} \left\{ D \int_0^1 \left(\theta\varphi + 2 \frac{\mathrm{d}\theta}{\mathrm{d}\eta} \right.\right.$$

$$\times \int_0^\eta \varphi \, \mathrm{d}\eta)(\theta + \bar{\theta}) \, \mathrm{d}\eta \int_0^a \frac{x}{\delta} \frac{\mathrm{d}\delta}{\mathrm{d}x} \mathrm{d}x$$

$$- aD \int_0^1 \frac{\mathrm{d}\theta}{\mathrm{d}\eta} (\theta + \bar{\theta}) \int_0^\eta \varphi \, \mathrm{d}\eta \, \mathrm{d}\eta - a \int_0^1 \frac{\mathrm{d}^2\theta}{\mathrm{d}\eta^2} \times (\theta + \bar{\theta}) \, \mathrm{d}\eta \Big\}, \quad (39)$$

where δ is variational symbol and θ, $\bar{\varphi}$ are defined as $\delta\theta/\delta\delta = \theta/\delta$ and $\delta\varphi/\delta\delta = \bar{\varphi}/\delta$. Equation (39) can be expressed after some rearrangement such that

$$\left(\frac{\delta \Phi}{\delta \delta'} \right)_{\delta'=\delta} = \frac{\rho\varkappa^3 Ra^* Pr}{a^3} \left\{ I_1(\theta, \varphi, \bar{\delta}_0) + \frac{qc_v}{T_\infty g\beta\lambda} I_2(\theta, \varphi, \bar{\delta}_0) \right\}, \quad (39)'$$

where

$$I_1 = \frac{D^3}{Pr} \int_0^1 \left(\varphi^2 - \frac{\mathrm{d}\varphi}{\mathrm{d}\eta} \int_0^1 \varphi \, \mathrm{d}\eta \right) (\bar{\varphi} - 2\varphi) \, \mathrm{d}\eta \times \int_0^1 \frac{\bar{x}^2}{\bar{\delta}^6} \left(1 - \frac{2\bar{x}}{\bar{\delta}} \frac{\mathrm{d}\bar{\delta}}{\mathrm{d}\bar{x}} \right) \mathrm{d}\bar{x} - \frac{2}{\int_0^1 \theta\varphi \, \mathrm{d}\eta}$$

$$\times \int_0^1 (\bar{\varphi} - 2\varphi) \int_\eta^1 \theta \, \mathrm{d}\eta \, \mathrm{d}\eta \int_0^1 \frac{\bar{x}}{\bar{\delta}} \frac{\mathrm{d}\bar{\delta}}{\mathrm{d}x} \mathrm{d}\bar{x} - D^2 \times \int_0^1 \frac{\mathrm{d}^2\varphi}{\mathrm{d}\eta^2} (\bar{\varphi} - 2\varphi) \, \mathrm{d}\eta \int_0^1 \frac{\bar{x}^2}{\bar{\delta}^6} \mathrm{d}\bar{x}, \quad (40)$$

$$I_2 = \frac{D}{(\mathrm{d}\theta/\mathrm{d}\eta)_0^2} \int_0^1 \left(\theta\varphi + 2 \frac{\mathrm{d}\theta}{\mathrm{d}\eta} \int_0^\eta \varphi \, \mathrm{d}\eta \right) (\theta + \bar{\theta}) \, \mathrm{d}\eta \times \int_0^1 \frac{\bar{x}}{\bar{\delta}} \frac{\mathrm{d}\bar{\delta}}{\mathrm{d}\bar{x}} \mathrm{d}\bar{x} - \frac{D}{(\mathrm{d}\theta/\mathrm{d}\eta)_0^2} \int_0^1 \frac{\mathrm{d}\theta}{\mathrm{d}\eta} (\theta + \bar{\theta}) \times \int_0^1 \varphi \, \mathrm{d}\eta \, \mathrm{d}\eta - \frac{1}{(\mathrm{d}\theta/\mathrm{d}\eta)_0^2} \int_0^1 \frac{\mathrm{d}^2\theta}{\mathrm{d}\eta^2} \times (\theta + \bar{\theta}) \, \mathrm{d}\eta.$$

I_1 is a monotonously increasing negative function of $\bar{\delta}_0$, while I_2 is a monotonously decreasing positive function of $\bar{\delta}_0$. Since the relation $qc_v/T_\infty g\beta\lambda \gg 1$ holds for ordinary conditions of the natural convection and the absolute values of I_1 is not so larger than that of I_2 at the neighbourhood of $\bar{\delta}_{0m}$, the sign of variational coefficient expressed by (39)′ is positive, and therefore Φ does not take minimum value but takes the smallest value at the minimum boundary layer thickness $\bar{\delta}_{0m}$. Inclusively, the solution obtained by the assumption of minimum boundary layer thickness gives the most plausible ones.

3. THE SOLUTION FOR A CIRCULAR PLATE

By denoting x-coordinate as a radial coordinate in Fig. 1, the basic equations of bound-

ary layer flow about the circular plate are expressed as follows;

$$\frac{\partial u}{\partial x}+\frac{\partial v}{\partial y}+\frac{u}{x}=0, \tag{41}$$

$$u\frac{\partial u}{\partial x}+v\frac{\partial u}{\partial y}=-\frac{1}{\rho}\frac{\partial p^*}{\partial x}+\nu\frac{\partial^2 u}{\partial y^2}, \tag{42}$$

$$0=-\frac{1}{\rho}\frac{\partial p^*}{\partial y}-g\beta(T-T_\infty), \tag{43}$$

$$u\frac{\partial T}{\partial x}+v\frac{\partial T}{\partial y}=\varkappa\frac{\partial^2 T}{\partial y^2}. \tag{44}$$

These equations are solved similarly as in the case of the infinite strip with the condition of the minimum boundary layer thickness as

$$\Delta_m^{\gamma'}-\Delta_m^6=\frac{n}{2}\left(1+\frac{1}{mPr}\right)\frac{\bar{x}^2}{\bar{\delta}_{0m}^6}, \tag{45}$$

where

$$\bar{\delta}_{0m}=\left[\frac{n(1+1/mPr)/2}{\Delta_{1m}^{\gamma'}-\Delta_{1m}^6}\right]^{\frac{1}{6}},$$

$$\Delta_{1m}=(3+2mPr)^{-1/(6-\gamma')}, \tag{46}$$

$$\gamma'=6/(3+2mPr) \tag{47}$$

and m, n are constants defined by (24).

Local Nusselt number Nu_x is given in the same form as that of (29) and average Nusselt number Nu is expressed as

$$Nu=\frac{qa}{\Delta T_{av}\lambda}=\left[\frac{-(\mathrm{d}\theta/\mathrm{d}\eta)_0}{2\bar{\delta}_{0m}\int_0^1\bar{x}\Delta_m\,\mathrm{d}\bar{x}}\right]^{\frac{1}{5}}(GrPr)^{\frac{1}{5}}, \tag{48}$$

where

$$\Delta T_{av}=2\int_0^a \Delta T_w\, x\,\mathrm{d}x/a^2, \tag{49}$$

and Gr is defined by (32).

4. THE SOLUTION FOR A RECTANGULAR PLATE

The coordinate system is shown in Fig. 1. The basic equations are

$$\frac{\partial u}{\partial x}+\frac{\partial v}{\partial y}+\frac{\partial w}{\partial z}=0, \tag{50}$$

$$u\frac{\partial u}{\partial x}+v\frac{\partial u}{\partial y}+w\frac{\partial u}{\partial z}=-\frac{1}{\rho}\frac{\partial p^*}{\partial x}+\nu\frac{\partial^2 u}{\partial y^2}, \tag{51}$$

$$u\frac{\partial w}{\partial x}+v\frac{\partial w}{\partial y}+w\frac{\partial w}{\partial z}=-\frac{1}{\rho}\frac{\partial p^*}{\partial z}+\nu\frac{\partial^2 w}{\partial y^2}, \tag{52}$$

$$0=-\frac{1}{\rho}\frac{\partial p^*}{\partial y}-g\beta(T-T_\infty), \tag{53}$$

$$u\frac{\partial T}{\partial x}+v\frac{\partial T}{\partial y}+w\frac{\partial T}{\partial z}=\varkappa\frac{\partial^2 T}{\partial y^2}. \tag{54}$$

In much the same way as the case of the infinite strip, the following similar profiles are assumed.

$$T-T_\infty=Q\theta(\eta)\delta,\quad \eta=y/\delta, \tag{11),(13}$$

$$u=u_{xz}(x,z)\varphi(\eta),\qquad v=v_{xz}(x,z)\varphi(\eta), \tag{55),(56}$$

where Q is defined by (14). When the following dimensionless variables are defined,

$$\left.\begin{aligned}&\bar{x}=x/a,\quad \bar{z}=z/a,\quad \bar{\delta}=\delta(Gr^*Pr)^{\frac{1}{5}}/a,\\&\bar{u}=u_{xz}a/(Gr^*Pr)^{\frac{1}{5}}\varkappa,\quad \bar{v}=v_{xz}a/(Gr^*Pr)^{\frac{1}{5}}\varkappa,\end{aligned}\right\} \tag{57}$$

the equations of momentum and energy integrated across the boundary layer are transformed after some rearrangement to

$$\frac{1}{Pr}\left\{\frac{\partial}{\partial\bar{x}}(\bar{\delta}\bar{u}^2)+\frac{\partial}{\partial\bar{z}}(\bar{\delta}\bar{u}\bar{w})\right\}=-A\frac{\partial\bar{\delta}^3}{\partial\bar{x}}-Y\frac{\bar{u}}{\bar{\delta}}, \tag{58}$$

$$\frac{1}{Pr}\left\{\frac{\partial}{\partial\bar{x}}(\bar{\delta}\bar{u}\bar{w})+\frac{\partial}{\partial\bar{z}}(\bar{\delta}\bar{w}^2)\right\}=-A\frac{\partial\bar{\delta}^3}{\partial\bar{z}}-B\frac{\bar{w}}{\bar{\delta}}, \tag{59}$$

$$\frac{\partial}{\partial\bar{x}}(\bar{\delta}^2\bar{u})+\frac{\partial}{\partial\bar{z}}(\bar{\delta}^2\bar{w})=D, \tag{60}$$

where A, B and D are constants defined by (19). It is difficult to obtain the analytical solution of (58), (59) and (60) for arbitrary Prandtl number.

4.1 *Analytical solution for infinite Prandtl number*

The left-hand side of (58) and (59) becomes negligibly small for $Pr\to\infty$. Substitution of $\bar{u}$ and $\bar{w}$ in these simplified equations into (60)

yields the following Poisson's equation

$$\frac{\partial \bar{\delta}^6}{\partial \bar{x}^2} + \frac{\partial \bar{\delta}^6}{\partial \bar{y}^2} = -\frac{2(\partial\theta/\partial\eta)_0^2 (\partial\varphi/\partial\eta)_0}{\int_0^1 \theta\varphi \, d\eta \int_0^1 d\eta \int_\eta^1 \theta \, d\eta} = -M. \quad (61)$$

The following boundary conditions may be assumable if the solutions of the infinite strip and the circular plate are taken into account;

$$\bar{x} = 0; \quad \partial\bar{\delta}/\partial\bar{x} = 0, \bar{z} = 0; \quad \partial\bar{\delta}/\partial\bar{z} = 0 \quad (62)$$

$$\bar{x} = \pm 1 \text{ and } \bar{z} = \pm L; \quad \bar{\delta} = 0, \quad (63)$$

where

$$L = b/a. \quad (64)$$

Equation (61) can be solved analytically as

$$\delta^6 = \frac{M}{2}\left[(1 - \bar{x}^2) - \frac{32}{\pi^3}\sum_{n=0}^{\infty} \times \frac{(-1)^n \cosh(n + 1/2)\pi z \cos(n + 1/2)\pi x}{(2n + 1)^3 \cosh(n + 1/2)\pi L}\right]. \quad (65)$$

Local Nusselt number Nu_{xz} is given in the same form as that of (29) and average Nusselt number Nu is expressed as

$$Nu = \frac{qa}{\Delta T_{av}\lambda} = \left[\frac{-(\partial\theta/\partial\eta)_0 L}{\int_0^1 \int_0^L \bar{\delta} \, d\bar{x} \, d\bar{z}}\right]^{\frac{1}{4}} (GrPr)^{\frac{1}{4}}, \quad (66)$$

where

$$\Delta T_{av} = \int_0^a \int_0^b \Delta T_w \, dx \, dz/ab, \quad (67)$$

and Gr is defined by (32).

4.2 *Approximate solution by Galerkin's method for arbitrary Prandtl number*

In order to apply Galerkin's method to the present problem it is necessary to deduce a differential equation, which contains only variable $\bar{\delta}$, by the appropriate rearrangement of (58), (59) and (60). Since this is not so accessible, except for the case of $Pr \to \infty$, simplified assumptions which satisfy (60) are introduced here,

$$\bar{\delta}^2\bar{u} = A_1\bar{x}, \quad (68)$$

$$\bar{\delta}^2\bar{w} = A_2\bar{z}, \quad (69)$$

$$A_1 + A_2 = D. \quad (70)$$

By multiplying (58) and (59) by $\bar{\delta}^6/\bar{x}$ and $\bar{\delta}^6/\bar{z}$ respectively and summing up the resultant equations,

$$\frac{1}{Pr}\left\{\frac{\bar{\delta}^6}{\bar{x}}\frac{\partial}{\partial\bar{x}}(\delta\bar{u}^2) + \frac{\bar{\delta}^6}{\bar{x}}\frac{\partial}{\partial\bar{z}}(\delta\bar{u}\bar{w}) + \frac{\bar{\delta}^6}{\bar{z}}\frac{\partial}{\partial\bar{x}}(\delta\bar{u}\bar{w}) + \frac{\bar{\delta}^6}{\bar{z}}\frac{\partial}{\partial\bar{z}}(\delta\bar{w}^2)\right\} = -A\left(\frac{\bar{\delta}^6}{\bar{x}}\frac{\partial\bar{\delta}^3}{\partial\bar{x}} + \frac{\bar{\delta}^6}{\bar{z}}\frac{\partial\bar{\delta}^3}{\partial\bar{z}}\right) - B\left(\frac{\bar{\delta}^5\bar{u}}{\bar{x}} + \frac{\bar{\delta}^5\bar{w}}{\bar{z}}\right). \quad (71)$$

By substituting (68), (69) and (70) into (71),

$$\left\{\frac{2(A_1^2 + A_1A_2 + A_2^2)}{Pr} + BD\right\}\bar{\delta}^3 - \frac{1}{Pr} \times \left\{(A_1^2 + A_1A_2)\bar{x}\frac{\partial\bar{\delta}^3}{\partial\bar{x}} + (A_1A_2 + A_2^2)\bar{z}\frac{\partial\bar{\delta}^3}{\partial\bar{z}}\right\} + \left(\frac{\bar{\delta}^6}{\bar{x}}\frac{\partial\bar{\delta}^3}{\partial\bar{x}} + \frac{\bar{\delta}^6}{\bar{z}}\frac{\partial\bar{\delta}^3}{\partial\bar{z}}\right) \doteq F(\bar{\delta}^3) = 0. \quad (72)$$

Boundary conditions may be assumed as

$$\bar{x} = 0; \quad \partial\bar{\delta}/\partial\bar{x} = 0, \bar{z} = 0; \quad \partial\bar{\delta}/\partial\bar{z} = 0, \quad (62)$$

$$\bar{x} = \pm 1; \quad \partial\bar{\delta}/\partial\bar{x} = \mp\infty, \bar{z} = \pm L; \quad \partial\bar{\delta}/\partial\bar{z} = \mp\infty. \quad (73)$$

The first approximation of the solution of (72) may be given by

$$\bar{\delta}^3(\bar{x}, \bar{z}) = a_1 + a_2(1 - \bar{x}^2)^{\frac{1}{2}}(L^2 - \bar{z}^2)^{\frac{1}{2}}, \quad a_1, a_2 \geqslant 0 \quad (74)$$

where a_1 and a_2 are to satisfy the following relation

$$\int_0^1 \int_0^L F(\bar{\delta}^3)(1 - \bar{x}^2)^{\frac{1}{2}}(L^{21} - \bar{z}^2)^{\frac{1}{2}} \, d\bar{x} \, d\bar{z} = 0. \quad (75)$$

By substituting (72) into (75),

$$\frac{2}{3}(La_2)a_1^2 + \left\{\frac{3\pi^2}{32}(La_2)^2 - \frac{\pi^2}{16}\frac{L^2}{1 + L^2}\right.$$

$$\times \left(\frac{A_1^2 + A_1A_2 + A_2^2}{A}\frac{2}{Pr} + \frac{BD}{A}\right)\Bigg\} a_1$$
$$+ \frac{16}{45}(La_2)^3 - \left\{\left(\frac{2}{9}\frac{D^2}{A} + \frac{8}{9}\frac{A_1^2 + A_1A_2 + A_2^2}{A}\right)\right.$$
$$\left.\times \frac{1}{Pr} + \frac{4}{9}\frac{BD}{A}\right\}\frac{L^2}{1+L^2}(La_2) = 0. \quad (76)$$

Two more conditions other than (70) and (76) are required for determining the values of a_1, a_2, A_1 and A_2. Then, the condition of minimum boundary layer thickness is employed, that is, a_1 and a_2 are determined so as to minimize δ at the plate center

$$\delta^3(0,0) = a_1 + La_2. \quad (77)$$

Thus,

$$A_1 = A_2 = D/2, \quad a_1 = 0,$$
$$a_2 = \left\{\frac{1}{1+L^2}\left(\frac{5}{2}\frac{D^2}{A}\frac{1}{Pr} + \frac{5}{4}\frac{BD}{A}\right)\right\}^{\frac{1}{3}}. \quad (78)$$

The boundary layer thickness and the average Nusselt number become

$$\bar{\delta}(\bar{x},\bar{z}) = \left\{\frac{1}{1+L^2}\left(\frac{5}{2}\frac{D^2}{A}\frac{1}{Pr} + \frac{5}{4}\frac{BD}{A}\right)\right\}^{\frac{1}{3}}$$
$$\times (1-\bar{x}^2)^{\frac{1}{3}}(L^2-\bar{z}^2)^{\frac{1}{3}}, \quad (79)$$

$$Nu = \left\{\frac{-4(\mathrm{d}\theta/\mathrm{d}\eta)_0}{B^2(\frac{1}{2},\frac{7}{6})}\right\}^{\frac{1}{3}}\left\{\frac{L^2}{1+L^2}\left(\frac{5}{2}\frac{D^2}{A}\frac{1}{Pr}\right.\right.$$
$$\left.\left.+\frac{5}{4}\frac{BD}{A}\right)\right\}^{-\frac{1}{3}}(GrPr)^{\frac{1}{3}}, \quad (80)$$

where $B(\frac{1}{2},\frac{7}{6})$ denotes a value of Beta function. In the case of the square plate these expressions are reduced to the following expressions

$$\bar{\delta}(\bar{x},\bar{z}) = \left(\frac{5}{4}\frac{D^2}{A}\frac{1}{Pr} + \frac{5}{8}\frac{BD}{A}\right)^{\frac{1}{3}}(1-\bar{x}^2)^{\frac{1}{3}}$$
$$\times (1-\bar{z}^2)^{\frac{1}{3}}, \quad (79)'$$

$$Nu = \left\{\frac{-4(\mathrm{d}\theta/\mathrm{d}\eta)_0}{B^2(\frac{1}{2},\frac{7}{6})}\right\}^{\frac{1}{3}}\left(\frac{5}{4}\frac{D^2}{A}\frac{1}{Pr} + \frac{5}{8}\frac{BD}{A}\right)^{-\frac{1}{3}}$$
$$\times (GrPr)^{\frac{1}{3}}. \quad (80)'$$

For the purpose of estimating the accuracy of the approximate solutions, those for the infinite strip and the circular plate are obtained as follows;
for the infinite strip,

$$\bar{\delta} = \left(\frac{5}{2}\frac{D^2}{A}\frac{1}{Pr} + \frac{BD}{A}\right)^{\frac{1}{3}}(1-\bar{x}^2)^{\frac{1}{3}}, \quad (81)$$

$$Nu = \left\{\frac{-2(\mathrm{d}\theta/\mathrm{d}\eta)_0}{B(\frac{1}{2},\frac{7}{6})}\right\}^{\frac{1}{3}}\left(\frac{5}{2}\frac{D^2}{A}\frac{1}{Pr} + \frac{BD}{A}\right)^{-\frac{1}{3}}$$
$$\times (GrPr)^{\frac{1}{3}}, \quad (82)$$

for the circular plate,

$$\bar{\delta} = \left(\frac{3}{4}\frac{D^2}{A}\frac{1}{Pr} + \frac{1}{2}\frac{BD}{A}\right)^{\frac{1}{3}}(1-\bar{x}^2)^{\frac{1}{3}}, \quad (83)$$

$$Nu = \{-\tfrac{7}{6}(\mathrm{d}\theta/\mathrm{d}\eta)_0\}^{\frac{1}{3}}$$
$$\times \left(\frac{3}{4}\frac{D^2}{A}\frac{1}{Pr} + \frac{1}{2}\frac{BD}{A}\right)^{-\frac{1}{3}}(GrPr)^{\frac{1}{3}}. \quad (84)$$

5. NUMERICAL RESULTS AND CONSIDERATIONS

Numerical evaluation of the solutions obtained in the preceding sections is made by assuming the following similar profiles of the temperature and velocity distribution within the boundary layer respectively,

$$\theta(\eta) = (1+\eta)(1-\eta)^3, \quad (85)$$
$$\varphi(\eta) = \eta(1-\eta)^3. \quad (86)$$

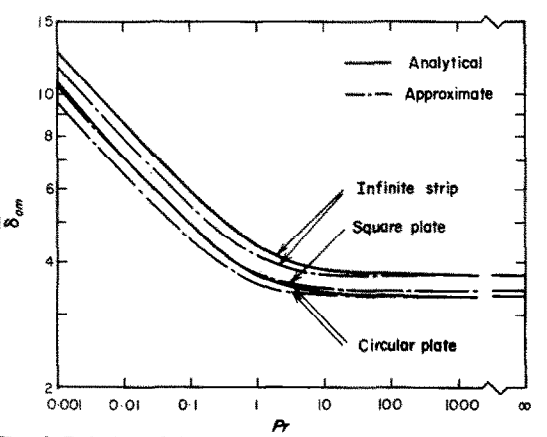

FIG. 2. Relation of the boundary layer thickness at the plate center δ_{0m} vs. Prandtl number Pr.

These satisfy boundary conditions (6) and (7). The experimental results by Aihara *et al.* [7] show that the temperature profile can be approximated fairly well by (85) except in the neighbourhood of the plate edges, and that the velocity profile outside of the maximum velocity point does not take any similarity, though the maximum velocity and the turning point of flow direction are in good agreement with the theoretical solution by Singh–Birkebak [17]. It is clarified, however, in the case of natural convection along a vertical surface [22] that the accuracy of these approximate profiles does not affect so seriously the heat transfer coefficient for moderate Prandtl number.

The values of dimensionless boundary-layer thickness at the plate center $\bar{\delta}_{0m}$ and average Nusselt number Nu for the infinite strip, the circular plate and the square plate are listed in Table 1.

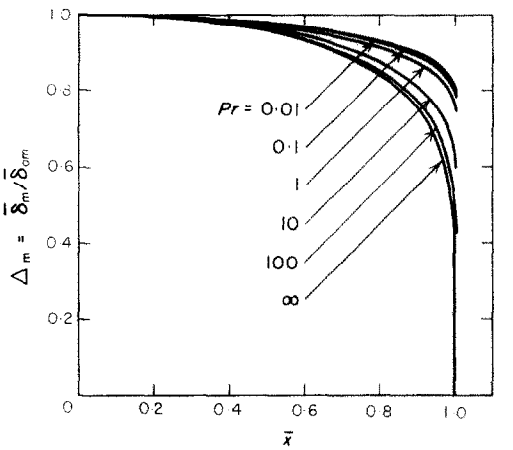

FIG. 3. Distribution of normalized boundary layer thickness along the infinite strip.

100. Figure 2 also gives a comparison made on the approximate solutions through Galerkin's method and the analytical ones. The former is 5–8 per cent smaller than the latter in the range

Table 1. *Boundary-layer thicknesses at the plate center* $\bar{\delta}_{0m}$ *and ratios of average Nusselt number to one-fifth power of Rayleigh number* $\mathrm{Nu/Ra^{\frac{1}{5}}}$

Pr		0·001	0·01	0·1	0·7	1	10	100	1000	∞
					Infinite strip					
$\bar{\delta}_{0m}$	analy.	12·60	8·60	5·93	4·56	4·39	3·86	3·76	3·75	3·74
	approx.	11·65	7·95	5·50	4·30	4·16	3·80	3·75	3·74	3·74
$Nu/Ra^{\frac{1}{5}}$	analy.	0·1152	0·1824	0·286	0·396	0·415	0·498	0·522	0·527	0·527
	approx.	0·1347	0·2135	0·332	0·447	0·463	0·518	0·526	0·527	0·527
					Circular plate					
$\bar{\delta}_{0m}$	analy.	10·45	7·13	4·94	3·88	3·76	3·40	3·34	3·34	3·34
	approx.	9·53	6·51	4·55	3·67	3·59	3·36	3·34	3·34	3·34
$Nu/Ra^{\frac{1}{5}}$	analy.	0·1503	0·2377	0·371	0·506	0·528	0·620	0·646	0·651	0·652
	approx.	0·1847	0·2917	0·449	0·581	0·597	0·645	0·651	0·651	0·652
					Square plate					
$\bar{\delta}_{0m}$	analy.	—	—	—	—	—	—	—	—	3·43
	approx.	10·38	7·09	4·92	3·90	3·79	3·50	3·47	3·46	3·46
$Nu/Ra^{\frac{1}{5}}$	analy.	—	—	—	—	—	—	—	—	0·644
	approx.	0·1735	0·2744	0·425	0·563	0·581	0·639	0·648	0·648	0·648

Figure 2 shows the relation of $\bar{\delta}_{0m}$ vs. Pr for the infinite strip, the circular plate and the square plate. The value of $\bar{\delta}_{0m}$ decreases gradually with the increase of Prandtl number up to $Pr = 100$, becoming almost constant in the range of $Pr >$ of $Pr < 1$, approaching the latter with the increase of Prandtl number. At the limit of $Pr \to \infty$, the approximate solutions for the infinite strip and the circular plate agree precisely with respective analytical ones, and the agree-

ment for the square plate is within one per cent.

In Fig. 3 is plotted as an example the distribution of normalized boundary layer thickness along the infinite strip $\Delta_m = \delta/\delta_{0m}$. The boundary layer thickness at the plate edge, i.e. at $\bar{x} = 1$, decreases with the increase of Prandtl number, approaching to zero at the limit of $Pr \to \infty$. The value of Δ_m through Galerkin's approximations is independent of Prandtl number and in accord with that of analytical solution for the case of $Pr \to \infty$.

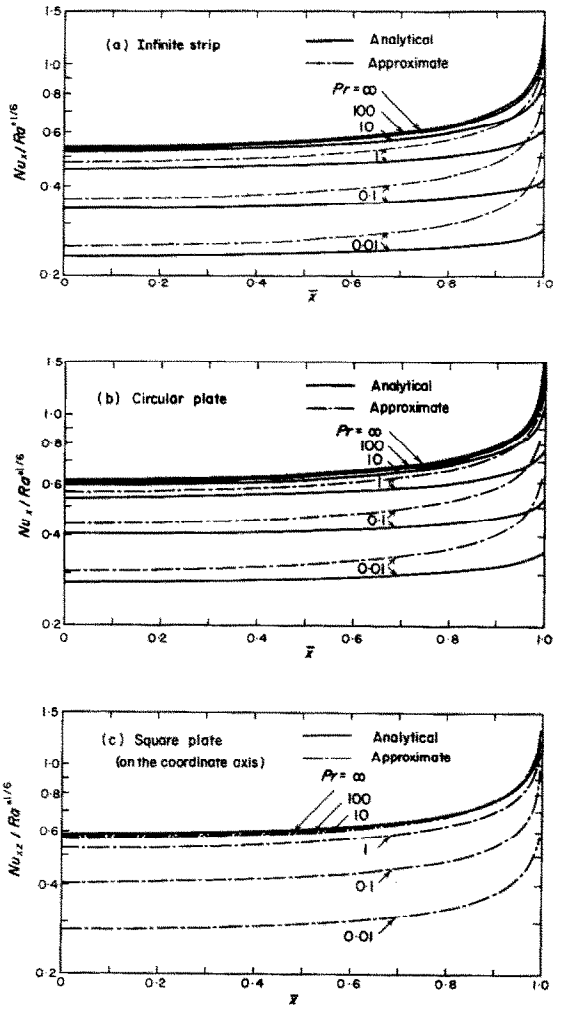

FIG. 4. Distribution of local Nusselt number. (a) Infinite strip, (b) Circular plate, (c) Square plate.

Figures 4(a), (b) and (c) show the distribution of local Nusselt number along the infinite strip, the circular plate and the square plate respectively. The approximate solution generally gives a higher local heat-transfer coefficient than analytical one, with their agreement getting worse in the neighbourhood of the plate edge. The former approaches to the latter with the increase of Prandtl number, and at the limit of $Pr \to \infty$ they agree completely with each other for the infinite strip and the circular plate and agree very well for the square plate. The tendencies of the present solutions shown in Figs. 2, 3 and 4(a) are similar to the results obtained by Clifton–Chapman [16] and Singh–Birkebak [17] for the case of the infinite strip with uniform wall temperature.

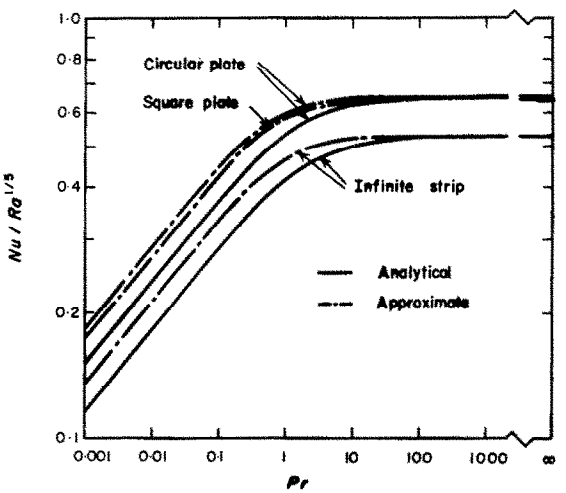

FIG. 5. Relation among average Nusselt number Nu, Rayleigh number Ra and Prandtl number Pr.

Figure 5 shows the relation of $Nu/Ra^{\frac{1}{4}}$ vs. Pr. The value of $Nu/Ra^{\frac{1}{4}}$ increases with the increase of Prandtl number up to $Pr = 100$, becoming almost constant in the range of $Pr > 100$, and it is higher in the order of the infinite strip, the square plate and the circular plate. The approximate solution takes a value about 10–20 per cent larger than the analytical one in the range of $Pr < 1$, approaching to the latter less than one

per cent in the range of $Pr > 100$. This relation between approximate and analytical solution seems to belong to a plate of arbitrary shape, to which Galerkin's method is applicable.

Figure 6 represents a comparison of the present solutions with the theoretical ones hitherto reported. In the solutions of Wagner [10], Singh *et al.* [15], Clifton–Chapman [16] and Singh–Birkebak [17] the following profiles are used,

$$\theta(\eta) = (1-\eta)^2, \quad \varphi(\eta) = \eta(1-\eta)^2, \qquad (87),(88)$$

and in Yamagata's [13]

$$\theta(\eta) = (1-\eta)^3, \quad \varphi(\eta) = \eta(1-\eta)^3. \qquad (89),(86)$$

The value of average Nusselt number by Singh–Birkebak is obtained by integrating graphically the local Nusselt numbers in Fig. 3 of [17]. All of these, except the authors', correspond to the case of uniform wall temperature. Figure 6 also shows the effect of assumed temperature and velocity profiles on the average Nusselt number. The values of $Nu/Ra^{\frac{1}{5}}$ obtained by the use of the profiles (85), (86) are about 4–7 per cent smaller than those by (87), (88) in the range of $Pr < 1$, and about 13 per cent in the range of $Pr > 100$. In Fig. 6 the value of $Nu/Ra^{\frac{1}{5}}$ for the infinite strip by Singh–Birkebak is about 10 per cent larger than that of the authors' in which the profiles (87), (88) are employed, though the assumptions made there are the same in principle. This difference seems to be due to the surface condition or correspondingly to the definition of the average heat transfer coefficient.

When the effect of assumed temperature and velocity profiles and surface conditions on the average heat-transfer coefficient are taken into account, the theoretical solutions for the infinite strip and the square plate, with uniform wall temperature and with uniform surface heat flux, will be included in the bands exhibited in Fig. 7 respectively. Experimental results hitherto reported are also plotted in Fig. 7, where the value of Aihara *et al.* is obtained by integrating graphically the local Nusselt numbers in Fig. 4 of [7], and that of Fishenden–Saunders [4] shows the value corrected by Stewartson [11]. The values of $Nu/Ra^{\frac{1}{5}}$ by Fishenden–Saunders, Birkebak–Abdulkadir [5] and Aihara *et al.* are about 10 per cent larger than theoretical ones. The experimental result by Fujii–Imura

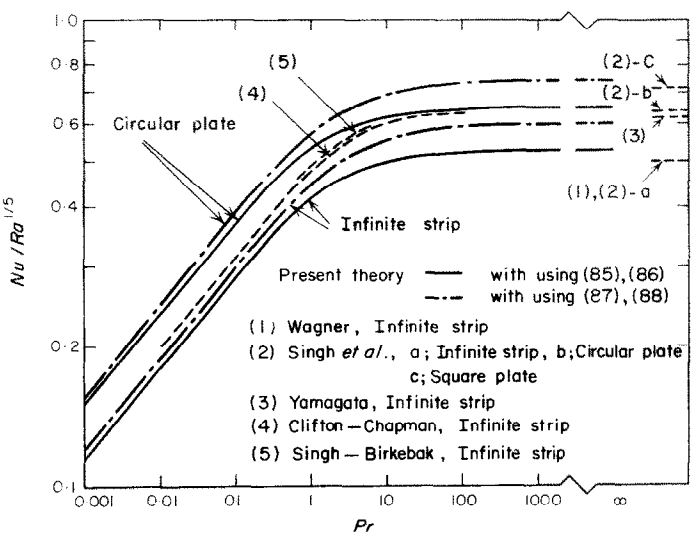

FIG. 6. Comparison among theoretical solutions on average Nusselt number.

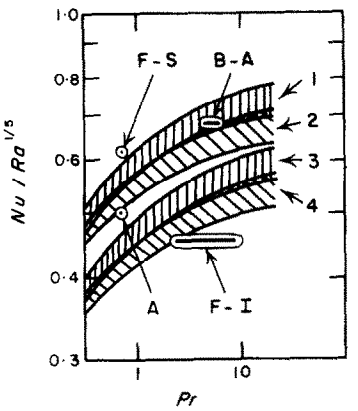

FIG. 7. Comparison between theoretical and experimental results on average Nusselt number.

	Experimental		
F–S	Fishenden–Saunders	Square	Uni. temperature
F–I	Fujii–Imura	Strip	Intermediate
B–A	Birkebak–Abdulkadir	Square	Uni. heat flux
A	Aihara *et al.*	Strip	Uni. temperature
	Theoretical		
1		Square	Uni. temperature
2		Square	Uni. heat flux
3		Strip	Uni. temperature
4		Strip	Uni. heat flux

[6] is about 10 per cent smaller than the theoretical value.

In the present theoretical study there remain uncertain the real profiles of temperature and velocity especially in the immediate neighbourhood of the plate edge, and the ratio of the boundary layer of temperature to that of velocity, which has more importance for a larger Prandtl number, and the range of Rayleigh number where the laminar boundary-layer approximation are applicable. Such uncertainty must be made clear by further experimental studies.

6. CONCLUSION

Laminar natural convection from heated horizontal plates with uniform surface heat flux facing downwards has been studied theoretically by an approximate integral treatment. The boundary layer equations are transformed into ordinary differential equations by integrating those across the boundary layer and by assuming similar profiles of temperature and velocity, as usual. The resulting set of equations are solved under the condition of minimum boundary-layer thickness. The principal results are summarized as follows;

(1) The condition of minimum boundary layer thickness, which is derived from the consideration on the time evolution of unsteady flow field by introducing the local potential of Gransdorf–Prigogine [20], is equivalent to the condition $|d\delta/dx| = \infty$ at plate edges, as proposed by Singh–Birkebak [17].

(2) Analytical solutions are obtained for the infinite strip and the circular plate. Local Nusselt numbers are shown in Figs. 4(a) and (b) respectively, and average Nusselt numbers in Table 1 and Fig. 5.

(3) At the limit of $Pr \to \infty$, the governing equations are transformed into Poisson's equation and the boundary layer thickness at the plate edge tends to zero. Consequently, it is not so difficult to obtain analytical solution for a plate of arbitrary shape. For example, the boundary layer thickness for a rectangular plate is expressed by (65), and the local Nusselt number on the coordinate axis of a square plate is shown in Fig. 4(c).

(4) Local Nusselt numbers obtained by Galerkin's approximate method for the infinite strip, the circular plate and the square plate are shown in Figs. 4(a), (b) and (c) respectively, and average Nusselt numbers in Table 1 and Fig. 5. Generally, the approximate solutions give higher heat-transfer coefficients than the analytical ones, and in the range of $Pr > 100$ they are in good agreement with each other.

(5) Local Nusselt number Nu_x, Nu_{xz} is proportional to one-sixth power of modified Grashof number, whereas average Nusselt number Nu is proportional to one-fifth power of Grashof number. The value of $Nu/Ra^{\frac{1}{5}}$ increases with the increase of Prandtl number up to $Pr = 100$, becoming almost constant in the range of $Pr > 100$ as shown in Fig. 6. Besides, it is the smallest for the infinite strip and becomes larger toward the rectangular plate and the circular plate.

(6) The average Nusselt number calculated is affected by the surface condition, that is, whether it is in uniform temperature or in uniform heat flux, and also by the assumed temperature and velocity profile. The experimental results hitherto reported are generally somewhat larger than theoretical ones. A more elaborate experimental study is required.

ACKNOWLEDGEMENTS

Present study was motivated by the discussion of current problems raised by Emeritus Professor K. Yamagata of Kyushu University. Associate Professor T. Murakami of Kyushu University helped the authors with useful discussions about introducing the concept of local potential. The authors wish to express their grateful acknowledgement to these persons. Numerical computations were performed with an electronic computer FACOM 230-60 in Computer Center, Kyushu University.

REFERENCES

1. R. WEISE, Wärmeübergang durch freie Konvektion an quadratischen Platten, *Forschung* **6**, 281–292 (1935).
2. O. A. SAUNDERS, M. FISHENDEN and H. D. MANSION, Some measurements on convection by an optical method, *Engineering* **139**, 483–485 (1935).
3. W. KRAUS, Temperatur—und Geschwidigkeitsfeld bei freier Konvection um eine waagerechte quadratische Platte, *Phys. Z.* **41**, 126–150 (1940).
4. M. FISHENDEN and O. A. SAUNDERS, *An Introduction to Heat Transfer*, p. 95. Clarendon Press, London (1950).
5. R. C. BIRKEBAK and A. ABDULKADIR, Heat transfer by natural convection from the lower side of finite horizontal, heated surface, *Heat Transfer 1970*, vol. IV, NC 2.2. Elsevier, Amsterdam (1970).
6. T. FUJII and H. IMURA, Natural-convection heat transfer from a plate with arbitrary inclination, *Int. J. Heat Mass Transfer* **15**, 755–767 (1972).
7. T. AIHARA, Y. YAMADA and S. ENDOO, Free convection from a heated, horizontal surface facing downwards (in Japanese), Proc. 8th Japan Heat Transfer Symp., Paper No. III-1.7, 325–328 (1971).
8. S. SUGAWARA and I. MICHIYOSHI, Heat transfer from a horizontal flat plate by natural convection (in Japanese), *Trans. Japan Soc. Mech. Engrs* **21**, 651–657 (1955).
9. S. LEVY, Integral methods in natural convection flow, *Trans. Am. Soc. Mech. Engrs* **22E**, 515–522 (1955).
10. C. WAGNER, Discussion on "Integral methods in natural convection flow", *Trans. Am. Soc. Mech. Engrs* **23E**, 320–321 (1956).
11. K. STEWARTSON, On the free convection from a horizontal plate, *Z. Angew. Math. Phys.* **9a**, 276–282 (1958).
12. W. N. GILL, D. W. ZEH and E. DEL CASAL, Free convection on a horizontal plate, *Z. Angew. Math. Phys.* **16**, 539–541 (1965).
13. K. YAMAGATA, Free convection from a horizontal surface (in Japanese), Proc. 6th Japan Heat Transfer Symp., No. II-1.4, 73–76 (1969).
14. Z. ROTEM, Free convection from heated, horizontal downward-facing plates, *Z. Angew. Math. Phys.* **21**, 472–475 (1970).
15. S. N. SINGH, R. C. BIRKEBAK and R. M. DRAKE, Laminar free convection heat transfer from downward-facing horizontal surfaces of finite dimensions, *Progress in Heat and Mass Transfer*, Vol. 2, p. 87. Pergamon Press, Oxford (1969).
16. J. V. CLIFTON and A. J. CHAPMAN, Natural-convection on a finite-size horizontal plate, *Int. J. Heat Mass Transfer* **12**, 1573–1584 (1969).
17. S. N. SINGH and R. C. BIRKEBAK, Laminar free convection from a horizontal infinite strip facing downwards, *Z. Angew. Math. Phys.* **20**, 454–461 (1969).
18. C. J. CHEN, Free convection from a two-dimensional finite horizontal plate, *Trans. Am. Soc. Mech. Engrs* **92C**, 548–550 (1970),
19. F. J. SURIANO and K. T. YANG, Laminar free convection about vertical and horizontal plates at small and moderate Grashof number, *Int. J. Heat Mass Transfer* **11**, 473–490 (1968).
20. P. GLANSDORFF and I. PRIGOGINE, On a general evolution criterion in macroscopic physics, *Physica* **30**, 351–374 (1964).
21. R. S. SCHECHTER and D. M. HIMMELBLAU, Local potential and system stability, *Physics Fluids* **8**, 1431–1437 (1965).
22. T. FUJII, Some considerations on the mathematical analysis of heat transfer from a veritcal flat surface by laminar free-convection (in Japanese), *Trans. Japan Soc. Mech. Engrs* **24**, 957–963 (1958).

UNE ETUDE THEORIQUE DU TRANSFERT THERMIQUE PAR CONVECTION NATURELLE A PARTIR DE SURFACES HORIZONTALES TOURNEES VERS LE BAS AVEC FLUX THERMIQUE UNIFORME

Résumé—Le texte présente une étude théorique de la convection naturelle laminaire stationnaire le long d'une plaque horizontale tournée vers le bas et chauffée à flux thermique uniforme. Les équations de la couche limite sont résolues par une méthode intégrale approchée, basée sur un concept d'épaisseur minimum de la couche limite qui est dérive de la considération de l'évolution dans le temps d'un champ d'écoulement non stationnaire.

Tandis que les solutions pour une bande infinie et une plaque circulaire sont obtenues analytiquement pour tout nombre de Prandtl, la solution pour une plaque rectangulaire est obtenue dans le seul cas de $Pr \to \infty$. On obtient aussi par la méthode de Galerkin des solutions approchées pour ces trois plaques. L'accord existant entre les solutions analytiques et approchées est bon, spécialement dans le cas où $Pr \to \infty$.

Le nombre local de Nusselt Nu_x est proportionnel à la puissance un sixième du nombre modifié de Grashof, alors que le nombre moyen de Nusselt Nu est proportionnel à la puissance un cinquième du nombre de Grashof. La valeur de $Nu/Ra^{1/5}$ croît avec le nombre de Prandtl jusqu'à $Pr = 100$ et devient pratiquement constante dans le domaine de $Pr > 100$. En outre, elle est la plus petite pour une bande infinie et devient plus grande pour des plaques rectangulaires et circulaires.

EINE THEORETISCHE UNTERSUCHUNG DER NATÜRLICHEN KONVEKTION BEI HORIZONTALEN FLÄCHEN MIT ABWÄRTSGERICHTETEM, GLEICHFÖRMIGEM WÄRMESTROM

Zusammenfassung—Die Arbeit behandelt die theoretische Untersuchung der stationären, laminaren natürlichen Konvektion an einer horizontalen Platte, die mit gleichmässigem Wärmestrom beheizt wird und nach unten zeigt. Die Grenzschichtgleichungen werden näherungsweise durch eine integrale Behandlung gelöst, die auf dem Prinzip eines Minimums der Grenzschichtdicke beruht, das aus der zeitlichen Entwicklung des instationären Strömungsfeldes abgeleitet ist. Die Lösungen für einen unendlichen Streifen und eine Kreisplatte erhält man analytisch für beliebige Prandtl-Zahlen, die für eine Rechteckplatte dagegen nur für $Pr \to \infty$. Für diese drei Platten erhält man auch Lösungen nach Galerkin's Methode. Die Übereinstimmung zwischen der analytischen und der Näherungslösung ist ziemlich gut, besonders für den Fall $Pr \to \infty$.

Die lokale Nusselt-Zahl ist proportional zur 1/6-Potenz der modifizierten Grashof-Zahl, die mittlere Nusselt-Zahl dagegen zur 1/5-Potenz der Grashof-Zahl. Der Wert von $Nu/Ra^{1/5}$ steigt mit der Prandtl-Zahl bis zu $Pr = 100$ an und wird für $Pr = 100$ fast konstant. Das Verhältnis ist für den unendlichen Streifen am kleinsten und wird fortschreitend grösser für die rechteckige Platte und die Kreisplatte.

ТЕОРЕТИЧЕСКОЕ ИССЛЕДОВАНИЕ ПЕРЕНОСА ТЕПЛА ЕСТЕСТВЕННОЙ КОНВЕКЦИЕЙ ОТ ОБРАЩЕННЫХ ВНИЗ ГОРИЗОНТАЛЬНЫХ ПОВЕРХНОСТЕЙ ПРИ ОДНОРОДНОМ ТЕПЛОВОМ ПОТОКЕ

Аннотация—Теоретически исследуется стационарное ламинарное течение (при естественной конвекции) вдоль горизонтальной обращенной поверхностью вниз пластины, нагреваемой однородным тепловым потоком. Уравнения пограничного слоя решаются с помощью приближенного интегрального метода, основанного на понятии минимальной толщины пограничного слоя, которая определяется из временной эволюции нестационарного поля потока.

В то время как для бесконечной полосы и круглой пластины аналитические решения получены для любых значений числа Прандтля, то для прямоугольной пластины решение получено только при $Pr \to \infty$. Для всех этих трех пластин найдены приближенные решения с помощью метода Галёркина. Аналитическое и приближенное решения дают хорошее совпадение особенно при $Pr \to \infty$.

Локальное число Нуссельта Nu_x пропорционально модифицированному числу Грасгофа в степени 1/6, а среднее число Нуссельта Nu пропорционально числу Грасгофа в степени 1/5. Значение $Nu/Ra^{1/5}$ увеличивается с увеличением значения числа Прандтля до $Pr = 100$, а потом становится почти постоянным при $Pr > 100$. Кроме того, это отношение является наименьшим для бесконечной пластины и увеличивается для прямоугольной и круговой пластин.